frontiers | Frontiers in Energy Research

TYPE Original Research
PUBLISHED 30 November 2023
DOI 10.3389/fenrg.2023.1328676

OPEN ACCESS

EDITED BY
Di Wang,
University of Ottawa, Canada

REVIEWED BY
Quantao Liu,
Wuhan University of Technology, China
Fan Zhang,
Aalto University, Finland

*CORRESPONDENCE
Zhengguang Wu,
zgwu@yzu.edu.cn

RECEIVED 27 October 2023
ACCEPTED 20 November 2023
PUBLISHED 30 November 2023

CITATION
Li B, Zhou Y, Wu Z, Kang A, Wu B and Luo C (2023), Influence of basalt fiber on performance of thin overlayer asphalt mixtures based on multiple experimental methods.
Front. Energy Res. 11:1328676.
doi: 10.3389/fenrg.2023.1328676

Influence of basalt fiber on performance of thin overlayer asphalt mixtures based on multiple experimental methods

Bo Li[1,2], Yangyang Zhou[1], Zhengguang Wu[1,2]*, Aihong Kang[1,2], Bangwei Wu[1,2] and Chufan Luo[1]

[1]College of Civil Science and Engineering, Yangzhou University, Yangzhou, China, [2]Research Center for Basalt Fiber Composite Construction Materials, Yangzhou, China

Because of the fast deterioration speed of the surface function of conventional asphalt pavement, thin overlayer with many advantages has been applied to the pavement surface. However, due to problems such as insufficient stripping resistance and cracking resistance, the performance of the thin overlayer needs to be further improved. To achieve this target, basalt fiber was introduced into two types of thin overlayer asphalt mixtures (Open graded friction course, OGFC-5, and Stone matrix asphalt mixture, SMA-5). The wheel tracking test and uniaxial penetration test for high temperature deformation resistance, low temperature bending beam test and indirect tensile asphalt (IDEAL) cracking test for cracking resistance, cantabro test for stripping resistance, and friction coefficient test for skid resistance were conducted to evaluate various performance of thin overlayer asphalt mixtures, along with the dynamic modulus test for dynamic mechanical response. The results showed that adding basalt fiber could enhance the high temperature deformation resistance, low temperature cracking resistance, intermediate temperature cracking resistance and stripping resistance of the thin overlayer, while having no significant impact on skid resistance. Furthermore, adding basalt fiber could increase the modulus in the high temperature region and decrease the modulus in the low temperature region of the thin overlayer asphalt mixtures, indicating thin overlayer with basalt fiber presenting superior both high temperature and low temperature performance. In addition, the evaluation indexes of S_{LT} and S_{HT} proposed from dynamic modulus test exhibited good consistency with the results of the performance tests.

KEYWORDS

thin overlayer asphalt mixture, basalt fiber, performance test, dynamic modulus, correlation analysis

1 Introduction

Due to long-term direct exposure to the external environment, suffering from the multiple influences of temperature fluctuation, rain erosion and vehicle load, the surface function of some asphalt pavements decays rapidly (Ding et al., 2022; Li et al., 2023; Yaqub et al., 2023). The thin overlayer has superior service performance, outstanding skid resistance and drainage performance, which not only enhances pavement service life, but also greatly

TABLE 1 Indexes of SBS modified asphalt.

Indexes		Results	Requirements
Softening point/°C		86	≥55
Penetration (25°C)/0.1 mm		71	60–80
Ductility (5 cm/min, 5°C)/cm		48	≥30
Recovery of elasticity (25°C)/%		76	≥65
RTFOT residue	Weight change/%	−0.08	±1.0
	Penetration ratio/%	86	≥60
	Residual ductility (15°C)/cm	37	≥20

improves the safety and comfort of the vehicle travel (Chen et al., 2019; Cui et al., 2021). In order to solve the problem of surface function deterioration, thin overlayer has been widely used in both new road construction and road maintenance projects (Correia and Zornberg, 2018; Almaali and Al-Busaltan, 2021; Jin T. et al., 2023).

However, the thin overlayer also has low durability due to its thin thickness and small aggregate particle size, which is manifested as insufficient cracking resistance, stripping resistance and high temperature deformation resistance (Ingrassia et al., 2012; Liu et al., 2019; Han et al., 2021). These problems limit further application of thin overlayer in pavement engineering. Huang et al. (2020) mixed cellulose fiber and basalt fiber into SMA and conducted experiments to determine the optimal mixing ratio. The findings indicated that the high temperature deformation resistance of the mixture increased with the increase of basalt fiber incorporation. The study conducted by Zhao et al. (2020) revealed that basalt fiber exhibited superior enhancement in the low temperature performance of asphalt mixture compared to lignin fiber and polyester fiber. As a new type of fiber commonly used in asphalt pavement surface layers, basalt fiber exhibits favorable reinforcement effect on asphalt mixtures, including significant enhancement in cracking resistance, rutting resistance and other performance (Zhang Y. et al., 2022; Zhang M. et al., 2022). Therefore, it can be considered that basalt fiber has great potential in improving the performance of thin overlayer, though few studies concerning this topic. Since a surface layer is directly subjected to the dynamic interaction of temperature and load, the dynamic mechanical response of the thin overlayer is also very important, in addition to the conventional experiments (Javilla et al., 2017; Jin et al., 2021; Liu et al., 2023). The dynamic modulus test was conducted using temperature and load frequency as environmental variables (Gudmarsson et al., 2015; Qin et al., 2019; Zhang C. et al., 2022), which gets closer to the realistic state than the conventional pavement performance test conditions. The master curve could be drawn, so that the dynamic modulus under extreme conditions could be predicted (Ling et al., 2017; Podolsky et al., 2018).

In this research, the influence of basalt fiber on the performance of OGFC-5 and SMA-5 was studied by multiple performance tests and dynamic modulus test. In addition, the results of dynamic modulus test and related performance tests (the wheel tracking test, uniaxial penetration test and low temperature bending beam test) were compared and analyzed.

TABLE 2 Indexes of basalt fiber.

Indexes	Results
Break strength/MPa	2,218
Break elongation/%	2.67
Elastic modulus/GPa	88
Acidity coefficient	5.3

TABLE 3 Indexes of lignin fiber.

Indexes	Results
Ash content/%	19.3
pH value	7.6
Asphalt absorption	6.2 m^a

[a]m is the mass of lignin fiber.

2 Materials and mixture design

2.1 Materials

In this research, SBS modified asphalt was selected. The performance tests of the asphalt were conducted with the Chinese standard of JTG E20-2011 (JTG, 2011), and the indexes are displayed in Table 1. The coarse and fine aggregates selected were all basalt aggregates.

The basalt fiber (BF) was used in OGFC and SMA, and lignin fiber (LF) was only used in SMA. The technical indexes of the fibers are displayed in Tables 2, 3, and the macroscopic appearances of the fibers are illustrated in Figure 1.

2.2 Mixture design

The OGFC-5 and SMA-5 gradations were selected for the asphalt mixture design, and the gradation curves of the two types of mixtures are displayed in Figure 2. There were four kinds of asphalt mixtures tested in this study, ordinary OGFC-5 without fiber, OGFC-5-BF with basalt fiber (0.3% by mixture mass), SMA-5 with only lignin fiber (0.3%), and SMA-5-BF with lignin fiber (0.1%) and basalt fiber (0.3%). The optimum asphalt content (OAC) and volumetric properties of the four asphalt mixtures, including voids in mineral aggregate (VMA), volume of air voids (VV), and voids filled with asphalt (VFA), are shown in Table 4.

3 Test methods

3.1 High temperature deformation resistance tests

3.1.1 Wheel tracking test

Wheel tracking test is usually conducted to test high temperature deformation resistance of mixtures. The test was conducted according to JTG E20-2011 (JTG, 2011), with three duplicates

10.3389/fenrg.2023.1328676

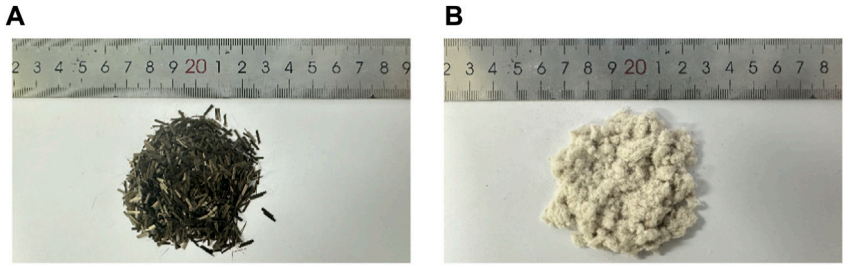

FIGURE 1
Macroscopic appearances of fibers: **(A)** Basalt fiber; **(B)** Lignin fiber.

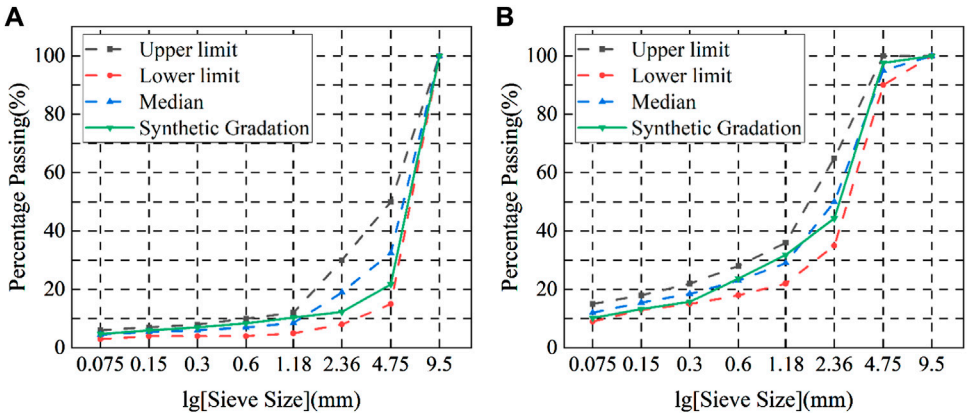

FIGURE 2
Gradation curves of asphalt mixtures: **(A)** OGFC-5; **(B)** SMA-5.

TABLE 4 Optimum asphalt content and volumetric properties of asphalt mixtures.

Types	OAC/%	VMA/%	VV/%	VFA/%
OGFC-5	5.0	27.5	19.6	28.7
OGFC-5-BF	5.1	27.3	19.3	29.3
SMA-5	6.5	17.3	4.0	76.9
SMA-5-BF	6.3	17.0	3.6	78.8

per group. The evaluation index is dynamic stability (*DS*), which is determined by Eq. 1.

$$DS = \frac{(t_2 - t_1) \times N}{d_2 - d_1} \times C_1 \times C_2 \quad (1)$$

in this equation, d_1 is the deformation depth corresponding to t_1 time (45 min), mm; d_2 is the deformation depth corresponding to t_2 time (60 min), mm; C_1 and C_2 are the test coefficients, in this study, $C_1 = C_2 = 1.0$; and N is the speed of the wheel, 42 cycles/min.

3.1.2 Uniaxial penetration test

Uniaxial penetration test is usually conducted to test high temperature deformation resistance of mixtures. The test was conducted according to JTG D50-2017 (JTG, 2017), with five duplicates per group. The evaluation index of shear strength (R_τ), can be determined by Eqs 2, 3.

$$\sigma_p = \frac{P}{A} \quad (2)$$

$$R_\tau = f_\tau \times \sigma_p \quad (3)$$

in this equation, σ_p is the penetration stress, MPa; P is the peak load of the specimen, N; A is the cross-sectional area of the pressing tool, mm^2; and f_τ is stress coefficient, which is 0.35.

3.2 Cracking resistance tests

3.2.1 Low temperature bending beam test

Low temperature bending beam test is usually conducted to test low temperature cracking resistance of mixtures. The test was conducted according to JTG E20-2011 (JTG, 2011), with four duplicates per group. The evaluation index is the failure strain (ε_B), which is determined by Eq. 4.

$$\varepsilon_B = \frac{6hd}{L^2} \quad (4)$$

in this equation, h is the height and L is the span of the specimen, mm; and d is the mid-span deflection of the specimen when damaged, mm.

3.2.2 IDEAL cracking test

IDEAL cracking test is usually conducted to test intermediate temperature cracking resistance of mixtures. The test was conducted according to ASTM D8225-19 (ASTM D8225-19, 2019), with three duplicates per group. The evaluation indexes are crack initiation work (W_S) and cracking tolerance index (CT_{index}), which are determined by Eqs 5, 6.

$$W_S = \int_0^{l_{100}} P dl \tag{5}$$

in this equation, P is the load, N; l is the displacement, mm; l_{100} is the displacement at peak load in the load-displacement curve.

$$CT_{index} = \frac{G_f}{|m_{75}|} \times \frac{l_{75}}{D} \tag{6}$$

in this equation, G_f is the fracture energy, J/m^2; l_{75} is the displacement at 75% peak load in the rear section of the load-displacement curve, mm; $|m_{75}|$ is absolute value of the rate of change at the 75% peak load in the rear section of the load-displacement curve, which is calculated by interpolation.

3.3 Stripping resistance test

Cantabro test is usually conducted to test stripping resistance of mixtures. The test was conducted according to JTG E20-2011 (JTG, 2011), with four duplicates per group. The specimens were firstly immersed in a water bath at 20°C for 20 h, and then put into the Los Angeles abrasion machine after being dried. The test was running for 10 min at the speed of 30 r/min. The evaluation index is the cantabro mass loss (ΔS), which is determined by Eq. 7.

$$\Delta S = \frac{m_0 - m_1}{m_0} \times 100 \tag{7}$$

in this equation, m_0 and m_1 are the total mass of the specimen before and after the cantabro test, g.

3.4 Skid resistance test

The friction coefficient (British pendulum number, *BPN*) test is usually conducted to test skid resistance of mixtures. The test was conducted according to JTG 3450-2019 (JTG, 2019), with three duplicates specimens per group. Each specimen was measured five times. The evaluation index is British pendulum number at 20°C (BPN_{20}), which is determined by Eq. 8.

$$BPN_{20} = BPN_T + \Delta BPN \tag{8}$$

in this equation, BPN_T is the British pendulum number corresponding to test temperature; ΔBPN is the temperature correction number.

The indexes of the performance tests are summarized in Table 5.

3.5 Dynamic modulus test

Dynamic modulus test was conducted according to JTG E20-2011 (JTG, 2011), and the compression dynamic modulus of mixtures was obtained. In this test, specimens with the diameter of 100 mm and height of 150 mm were prepared, with four duplicates in each group. The dynamic modulus test procedures are roughly displayed in Figure 3.

TABLE 5 Evaluation indexes of conventional performance tests.

Tests	Indexes	Units
Wheel tracking test	*DS*	cycles/mm
Uniaxial penetration test	R_t	MPa
Low temperature bending beam test	ε_B	με
IDEAL cracking test	W_S	J
	CT_{index}	/
Cantabro test	ΔS	%
Friction coefficient test	BPN_{20}	/

Asphalt mixture has the time-temperature equivalence property. Thus, dynamic modulus measured at other temperatures can be converted to the reference temperature (normally 20°C) by shift factor $\alpha(T)$ (Tan et al., 2020). Finally, the dynamic modulus master curve founded on the Sigmoidal function can be formed with the reference of NCHRP 9-29, so as to evaluate mechanical performance of mixtures. Sigmoidal function is shown in Eqs 9–13.

$$\lg|E^*| = \delta + \frac{|E^*|_{max} - \delta}{1 + e^{\beta + \gamma \lg \omega_r}} \tag{9}$$

in this equation, $|E^*|$ is the dynamic modulus of specimen, MPa; $|E^*|_{max}$ is the maximum dynamic modulus, MPa; ω_r is the reduced frequency, Hz; and δ,β, and γ are fitting parameters. $|E^*|_{max}$ is determined by Hirsch model, as shown in Eq. 10.

$$|E^*|_{max} = P_c\left[4200000\left(1 - \frac{VMA}{100}\right) + 435000\left(\frac{VFA \cdot VMA}{10000}\right)\right] + \frac{1 - P_c}{\left[\frac{\left(1 - \frac{VMA}{100}\right)}{4200000} + \frac{VMA}{435000VFA}\right]} \tag{10}$$

where P_c is an intermediate variable in the model calculation process, which is determined by Eq. 11.

$$P_c = \frac{\left(20 + \frac{435000VFA}{VMA}\right)^{0.58}}{650 + \left(\frac{435000VFA}{VMA}\right)^{0.58}} \tag{11}$$

where VMA and VFA are the volumetric properties of the specimen, %.

ω_r is the reduced frequency, which is to convert loading frequency at different temperatures into the frequency at the reference temperature by shift factor. The conversion between loading frequency and reduced frequency is determined by Arrhenius equation, as displayed in Eqs 12, 13.

$$\lg\omega_r = \lg\omega + \lg\alpha(T) \tag{12}$$

$$\lg\alpha(T) = \frac{\Delta E_a}{19.14714}\left(\frac{1}{T + 273.15} - \frac{1}{T_r + 273.15}\right) \tag{13}$$

where ω is the loading frequency, Hz; T is the test temperature, °C; T_r is the reference temperature, °C; and ΔE_a is the activation energy, which is a fitting parameter.

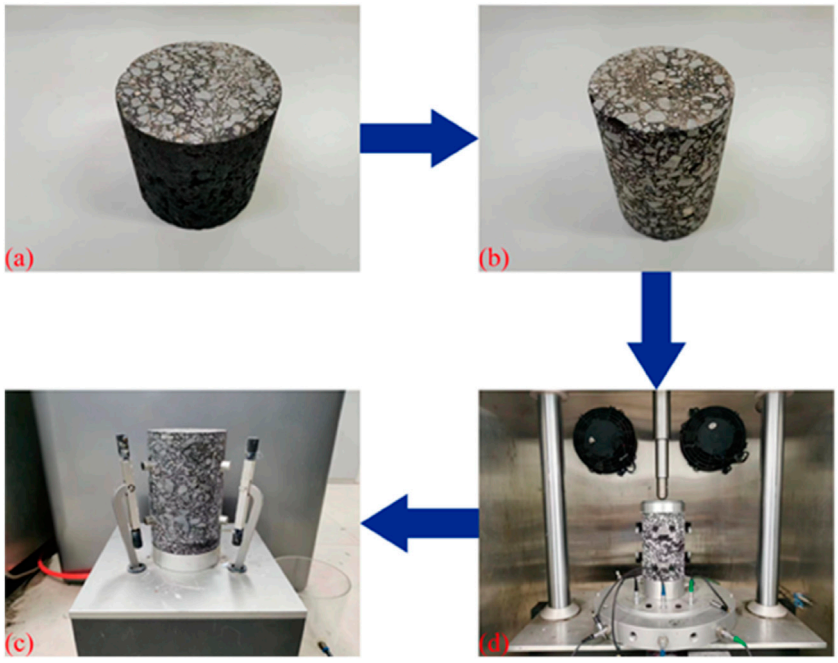

FIGURE 3
The dynamic modulus test procedures: **(A)** Specimen preparation; **(B)** Core sample drilling; **(C)** Sensor installation; **(D)** Testing.

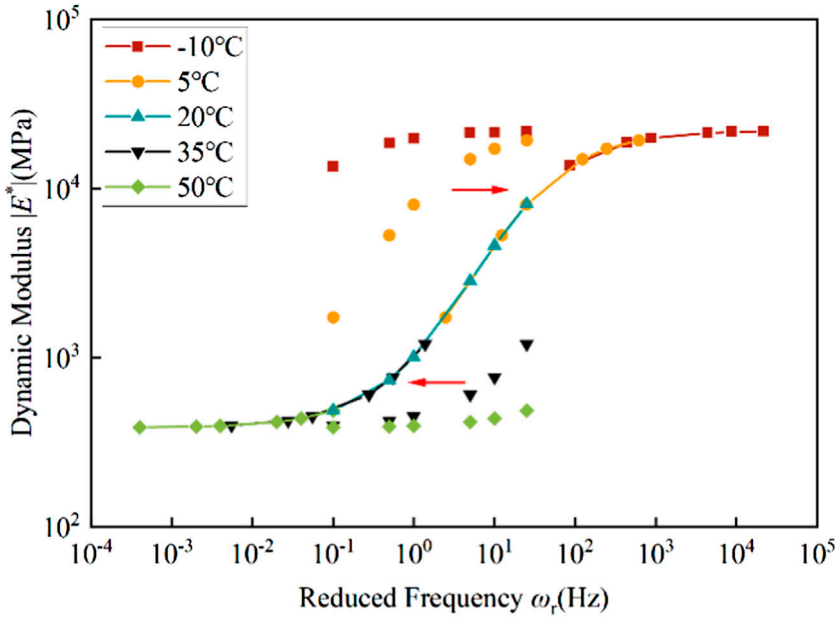

FIGURE 4
Shift process of each part of the loading frequency section.

The converting process of the master curve is illustrated in Figure 4. It can be seen from Figure 4 that the high frequency section was obtained by shifting the low temperature parts of the loading frequency section, while the low frequency section was obtained by shifting the high temperature parts of the loading frequency section. Hence, the high frequency section of the mater curve reflects the low temperature performance of mixtures while the low frequency section reflects the opposite.

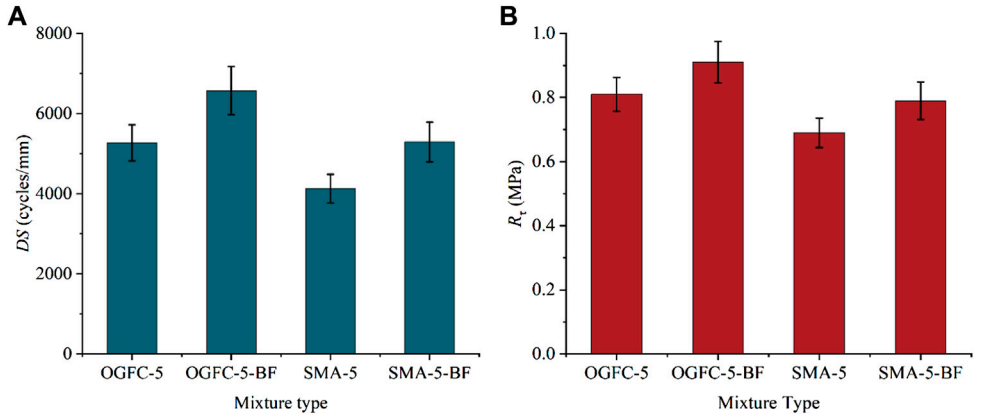

FIGURE 5
The results of high temperature deformation resistance tests: **(A)** *DS*; **(B)** R_{τ}.

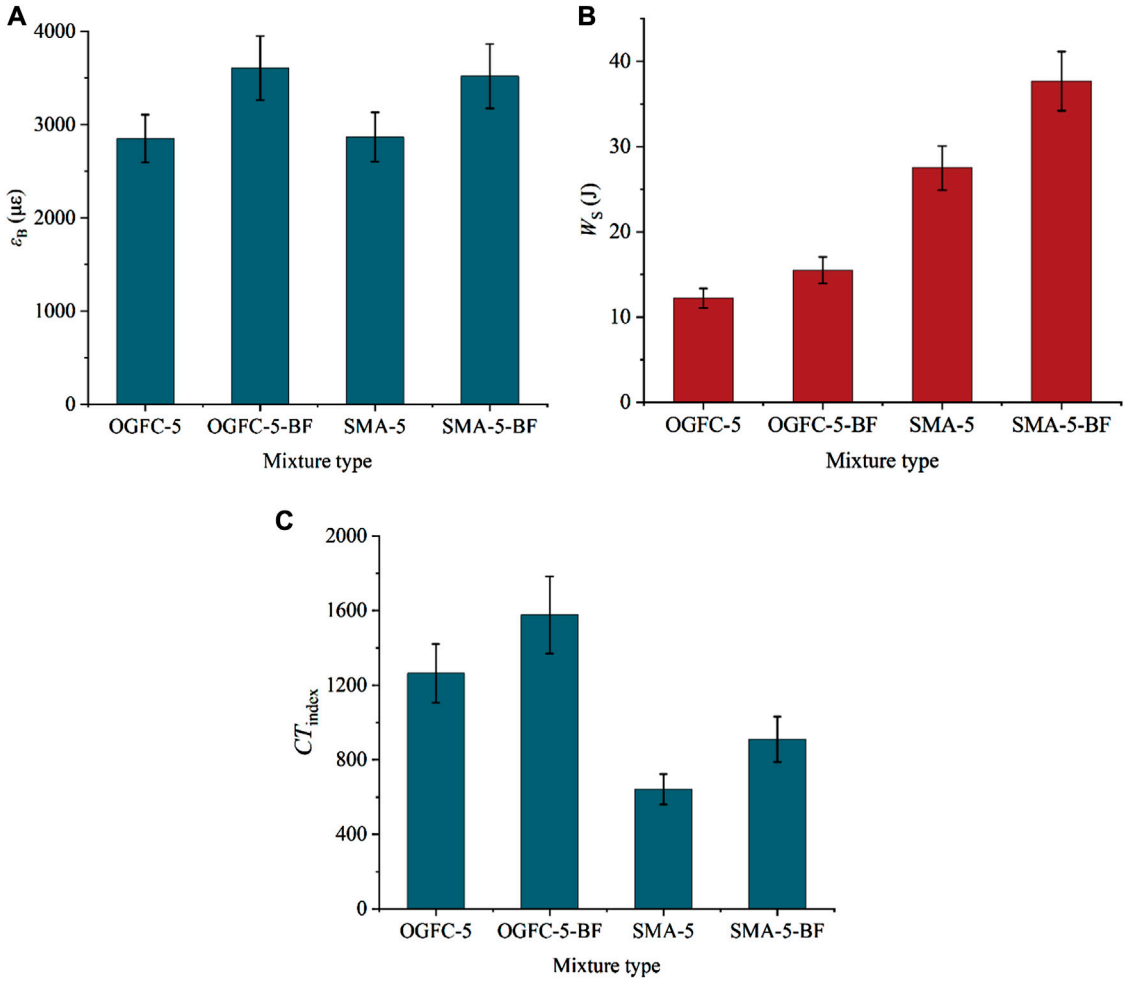

FIGURE 6
The results of cracking resistance tests: **(A)** ε_B; **(B)** W_S; **(C)** CT_{index}.

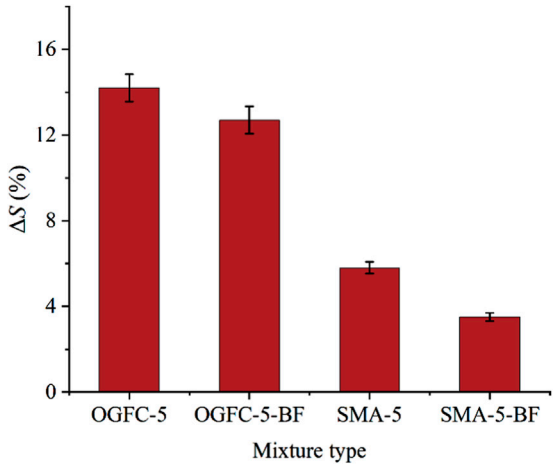

FIGURE 7
The results of stripping resistance test.

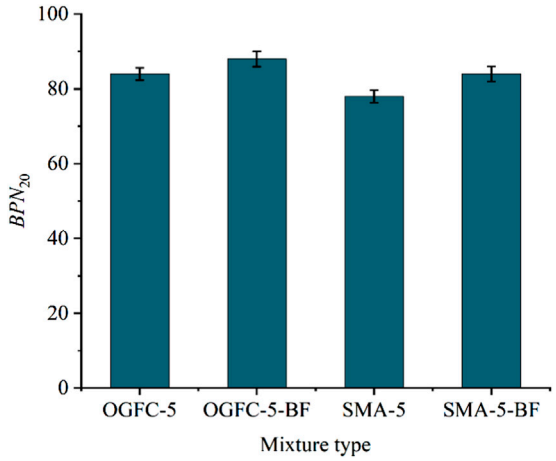

FIGURE 8
The results of skid resistance test.

4 Results and discussion

4.1 High temperature deformation resistance

DS and R_τ characterize high temperature deformation resistance of mixtures. As seen in Figures 5A, B, after adding basalt fiber, *DS* and R_τ of OGFC-5 increased by 24.7% and 12.3% respectively, while those of SMA-5 increased by 28.1% and 14.5% respectively. The results refer that adding basalt fiber could enhance the high temperature deformation resistance of the two thin overlayer asphalt mixtures, though a slightly greater enhancement could be observed on SMA-5 than OGFC-5. This phenomenon might be attributed to the fact that the addition of fiber could enhance the modulus of asphalt binder (Lou et al., 2022; Xie and Wang, 2023), thereby reducing the internal flow deformation of thin overlayer asphalt mixtures at high temperatures.

4.2 Cracking resistance

ε_B characterizes low temperature cracking resistance of mixtures. As seen in Figure 6A, after adding basalt fiber, ε_B of OGFC-5 and SMA-5 increased by 26.4% and 22.7% respectively. The results refer that adding basalt fiber could enhance the low temperature cracking resistance of the two thin overlayer asphalt mixtures, though a slightly greater enhancement could be observed on OGFC-5 than SMA-5. In addition, it can be found that ε_B values of OGFC-5 and SMA-5 (or OGFC-5-BF and SMA-5-BF) were at the same level, indicating the two types of mixtures demonstrated the approximate low temperature cracking resistance. Zhao et al. (2020) found that the addition of basalt fiber, lignin fiber and polyester fiber could enhance the low temperature cracking resistance of asphalt mixture to different degrees. Among these fibers, basalt fiber demonstrated the optimal improvement effect.

W_S and CT_{index} characterize intermediate temperature cracking resistance of mixtures. W_S reflects the resistance of crack formation, and CT_{index} reflects the resistance of crack expansion. As seen in Figures 6B, C, after adding basalt fiber, W_S and CT_{index} of OGFC-5 increased by 26.7% and 24.8% respectively, while those of SMA-5 increased by 37.1% and 41.7% respectively. The results indicate that adding basalt fiber could increase the intermediate temperature cracking resistance of the two thin

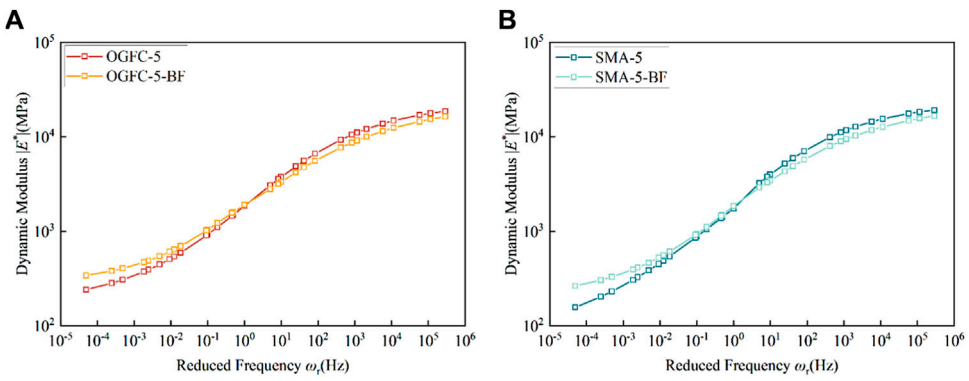

FIGURE 9
The results of dynamic modulus test: **(A)** Master curves of OGFC-5 and OGFC-5-BF; **(B)** Master curves of SMA-5 and SMA-5-BF.

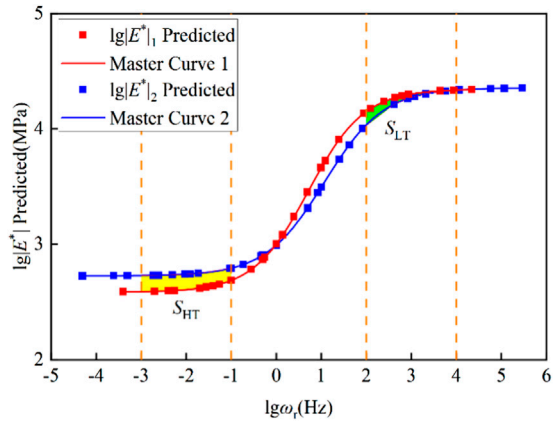

FIGURE 10
Schematic diagram of S_{LT} and S_{HT} calculation.

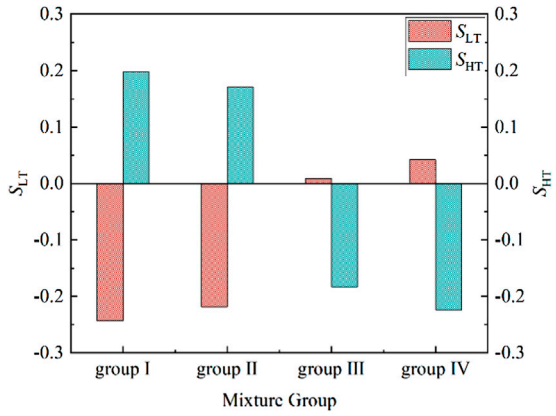

FIGURE 11
Calculation results of S_{LT} and S_{HT}.

overlayer asphalt mixtures, and a greater enhancement could be observed on SMA-5 than OGFC-5. This phenomenon might be attributed to the fact that the addition of fiber could enhance the toughness of asphalt binder (Wang et al., 2023; Xie and Wang, 2023), thereby delaying the cracking of thin overlayer asphalt mixtures at low and intermediate temperature. Furthermore, due to the lower volume of air voids (VV) and higher voids filled with asphalt (VFA) in SMA-5, the reinforcing effect of fiber in its asphalt binder was more pronounced, resulting in superior enhancement effect of intermediate temperature cracking resistance.

4.3 Stripping resistance

ΔS characterizes stripping resistance of mixtures. As seen in Figure 7, after adding basalt fiber, ΔS of OGFC-5 and SMA-5 decreased by 10.6% and 39.7% respectively. The results present that adding basalt fiber could strengthen the stripping resistance of the two thin overlayer asphalt mixtures, and a greater enhancement could be

TABLE 6 Grouping of asphalt mixtures.

Groups	Group I	Group II	Group III	Group IV
Mixture 1	OGFC-5	SMA-5	OGFC-5	OGFC-5-BF
Mixture 2	OGFC-5-BF	SMA-5-BF	SMA-5	SMA-5-BF

TABLE 7 Values of the index vectors.

Index vectors	X_1	X_2	X_3	X_4	X_5
Corresponding indexes	*DS*	R_τ	ε_B	S_{LT}	S_{HT}
x_{i1}	1,302	0.10	754	−0.243	0.198
x_{i2}	1,161	0.10	650	−0.218	0.171
x_{i3}	−1,142	−0.12	17	0.009	−0.183
x_{i4}	−1,283	−0.12	−87	0.042	−0.224

TABLE 8 Results of the correlation coefficients.

Groups	(X_1, X_5)	(X_2, X_5)	(X_3, X_4)
Results	0.9994	0.9960	−0.9995

observed on SMA-5 than OGFC-5. Zhang et al. (2020) observed that basalt fiber, polyester fiber and polyacrylonitrile fiber could effectively improve the stripping resistance of OGFC mixture, and the enhancement effect was superior when the basalt fiber content was between 0.15% and 0.30%. This phenomenon might be due to that the addition of fiber could increase the adhesion effect between asphalt binder and aggregates (Pei et al., 2021; Guo et al., 2023), thereby strengthening the overall integrity of thin overlayer asphalt mixtures.

4.4 Skid resistance

BPN_{20} (20°C) characterizes skid resistance of mixtures. As seen in Figure 8, after adding basalt fiber, BPN_{20} of OGFC-5 and SMA-5 only increased by 4.8% and 7.7% respectively. It means that adding basalt fiber presented no obvious effect on the skid resistance of the two mixtures, the reason might be that the addition of fibers caused hardly changes on the surface microtexture of thin overlayer asphalt mixtures, which is the key factor affecting the skid resistance (Xue et al., 2022). The addition of basalt fiber could only slightly change the surface macrotexture of mixtures, and the contribution to the improvement of skid resistance was very small, resulting in very limited enhancement effect.

4.5 Dynamic mechanical response

By the method described in the Section 3.5, the measured dynamic modulus data of OGFC-5, OGFC-5-BF, SMA-5, and SMA-5-BF were respectively fitted to master curves, which are displayed in Figure 9.

Asphalt mixtures present both elastic and viscous characteristics. The mixture is mainly elastic at low temperature and viscous at high temperature, which is primarily due to the complexity of the asphalt (Büchner et al., 2019; Jin D. et al., 2023). The mixture is prone to cracking

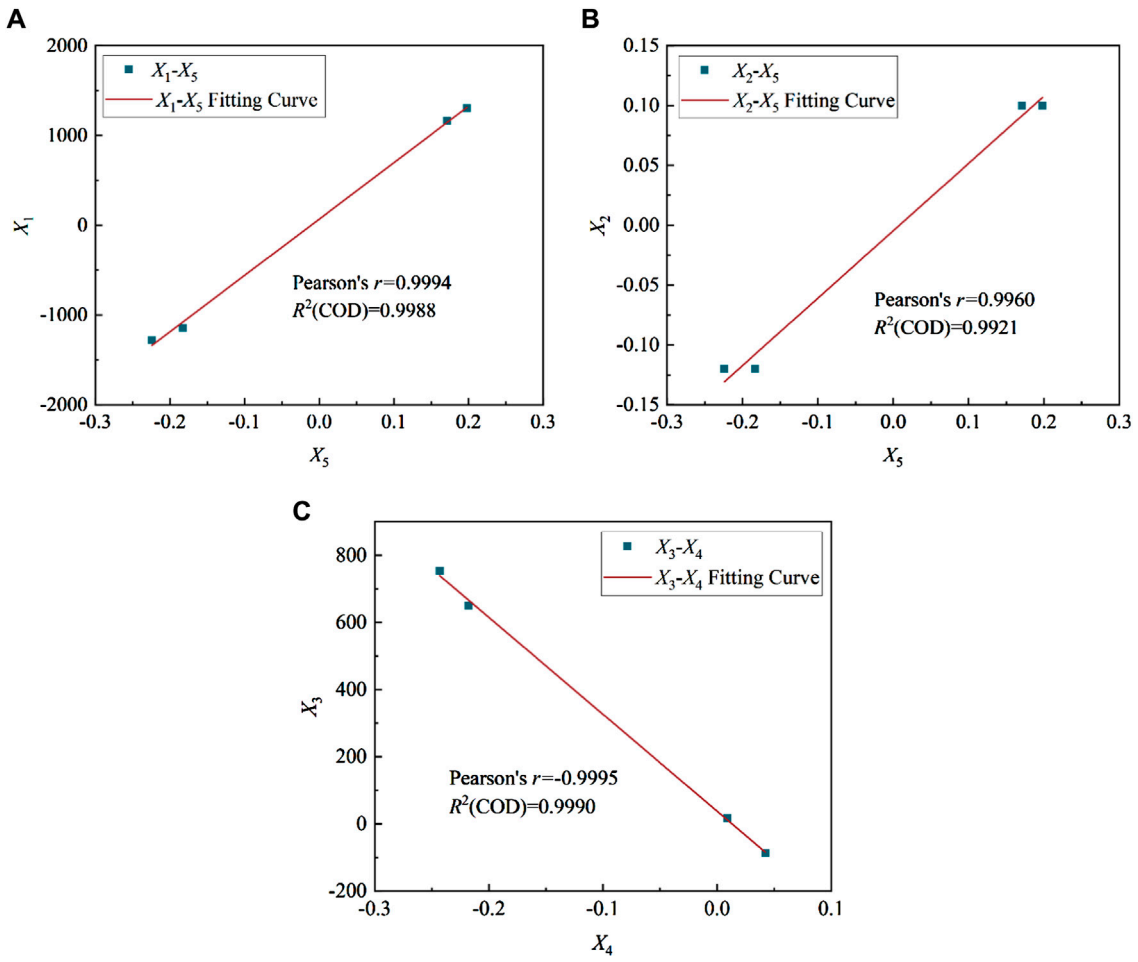

FIGURE 12
Two-dimensional distribution diagrams of the index vector groups: **(A)** (X_1, X_5); **(B)** (X_2, X_5); **(C)** (X_3, X_4).

at low temperature and excellent deformation ability is essential. Therefore, smaller modulus of the mixture should be desirable at low temperature. The mixture is prone to rutting at high temperature and good resistance to deformation is necessary. Subsequently, bigger modulus of the mixture should be desirable at high temperature. As shown in Figure 9, for both types of mixtures, adding basalt fiber could decrease the dynamic modulus of high frequency (low temperature) region, and increase the dynamic modulus of low frequency (high temperature) region.

In order to quantitatively analyze the dynamic modulus changes of mixtures caused by basalt fiber, the indexes S_{LT} and S_{HT} were introduced. S_{LT} and S_{HT} are determined by Eqs 14, 15, and the calculation diagram is displayed in Figure 10.

$$S_{LT} = \int_{2}^{4} \left(\lg|E^*|_2 - \lg|E^*|_1\right) \mathrm{d}\left(\lg\omega_r\right) \tag{14}$$

$$S_{HT} = \int_{-3}^{-1} \left(\lg|E^*|_2 - \lg|E^*|_1\right) \mathrm{d}\left(\lg\omega_r\right) \tag{15}$$

S_{LT} and S_{HT} are relative indexes. When $S_{LT} < 0$, it means low temperature performance of mixture 2 is greater than that of mixture 1. When $S_{HT} > 0$, it means high temperature performance of mixture 2 is greater than that of mixture 1. The four mixtures were divided into the following groups for analysis, as shown in Table 6.

The S_{LT} and S_{HT} indexes of the four groups of mixtures were calculated respectively and the results are illustrated in Figure 11.

It was found from Figure 11 that the S_{LT} values of mixtures in group I and group II were all negative. It meant that adding basalt fiber could decease the modulus in low temperature region, resulting in superior low temperature cracking resistance for both of the mixtures. Besides, the S_{LT} values of mixtures in group III and group IV were closer to zero, indicating the low temperature performance of OGFC-5 and SMA-5 was roughly the same. On the opposite, the S_{HT} values of mixtures in group I and group II were all positive. It referred that adding basalt fiber caused an increase in the modulus in high temperature region, which was also desirable to improve the high temperature deformation resistance. In addition, the S_{HT} values of mixtures in group III and group IV were also negative, indicating that the high temperature deformation resistance of OGFC-5 was better than that of SMA-5, which was accordance with the high temperature performance test results. Overall, after adding basalt fiber, the dynamic modulus of the two types of mixtures decreased in the high frequency (low temperature) section and increased in the low frequency (high temperature) section, reflecting that adding basalt fiber could enhance both of the low temperature and high temperature performance of mixtures.

4.6 Comparative analysis

Based on the correlation analysis, the consistency of the indexes S_{LT} and S_{HT} with the performance test indexes was investigated. The degree of correlation is determined by the Pearson correlation coefficient, as expressed by Eq. 16.

$$r = \frac{Cov(X_i, X_j)}{\sigma_i \sigma_j} = \frac{\sum(X_i - \overline{X_i})(X_j - \overline{X_j})}{\sqrt{\sum(X_i - \overline{X_i})^2 \sum(X_j - \overline{X_j})^2}} \quad (16)$$

where X_i and X_j are index vectors.

Before analyzing the correlation, the index vectors needed to be constructed. The groups used in dynamic modulus test were also used herein. The index vector X_1 corresponded to the index *DS* of the wheel tracking test, the index vector X_2 corresponded to the index R_τ of the uniaxial penetration test, the index vector X_3 corresponded to the index ε_B of the low temperature bending beam test, the index vector X_4 corresponded to the index S_{LT} introduced in the dynamic modulus test, and the index vector X_5 corresponded to the index S_{HT} introduced in the dynamic modulus test. The values of the index vectors are displayed in Table 7.

Correlation analysis was performed through combining (X_1, X_5), (X_2, X_5), and (X_3, X_4), and the correlation coefficient results are displayed in Table 8.

As can been seen from Table 8 that the three index vector groups of (X_1, X_5), (X_2, X_5), and (X_3, X_4) were all highly correlated, and the correlation coefficients were all above 0.9960. The results showed that the index *DS* and R_τ showed a great correlation degree with index S_{HT}, and the index ε_B presented a great correlation degree with index S_{LT}. By analyzing the two-dimensional distribution of the three groups, the evaluation consistency was further studied. The two-dimensional distribution diagrams are shown in Figure 12. It can be observed from Figure 12 that, the (X_1, X_5) and (X_3, X_4) groups had a strong linear correlation, all data points basically fell on the fitting curve with the R^2 above 0.9980. The linear correlation of (X_2, X_5) group was slightly weaker, and the data points had a certain fluctuation from the fitting curve with the R^2 around 0.9920. Overall, the two evaluation indexes introduced in the dynamic modulus test were exactly consistent with the performance test indexes, which could be used to predict and characterize high temperature and low temperature performance of thin overlayer mixtures.

5 Conclusion

In this research, the influence of basalt fiber on the performance of the thin overlayer was studied by multiple performance tests and the dynamic modulus test. In addition, the consistency between the introduced indexes (S_{LT} and S_{HT}) and the evaluation indexes in performance tests was analyzed. The conclusions are as follows:

(1) Adding basalt fiber can increase *DS* and R_τ presenting high temperature deformation resistance by around 26% and 13% respectively, increase ε_B presenting low temperature cracking resistance by around 24%, and increase W_S and CT_{index} presenting intermediate temperature cracking resistance by more than 26% and 24% respectively of thin overlayer mixtures.
(2) Adding basalt fiber can enhance stripping resistance, but causes no obvious influence on skid resistance of thin overlayer mixtures.
(3) Adding basalt fiber can decrease dynamic modulus in the high frequency section and increase it in the low frequency section, indicating both low temperature and high temperature performance of thin overlayer mixtures can be improved.
(4) The results of the dynamic modulus test and performance tests demonstrate good consistency. The indexes S_{LT} and S_{HT} can be used to evaluate low temperature and high temperature performance of thin overlayer mixtures.

In future research, more test methods can be used to study the influence of basalt fiber on the performance of the thin overlayer. In addition, the influence of fiber type on the performance of the thin overlayer also need to be further studied.

Data availability statement

The raw data supporting the conclusion of this article will be made available by the authors, without undue reservation.

Author contributions

BL: Conceptualization, Formal Analysis, Methodology, Project administration, Visualization, Writing–original draft. YZ: Data curation, Formal Analysis, Investigation, Methodology, Visualization, Writing–original draft. ZW: Conceptualization, Formal Analysis, Project administration, Supervision, Writing–review and editing. AK: Conceptualization, Funding acquisition, Methodology, Project administration, Supervision, Writing–review and editing. BW: Formal Analysis, Funding acquisition, Methodology, Project administration, Writing–review and editing. CL: Investigation, Methodology, Visualization, Writing–original draft.

Funding

The author(s) declare financial support was received for the research, authorship, and/or publication of this article. This research was funded by the National Natural Science Foundation of China, Grant Numbers 52008365 and 52178439. In addition, this research was funded by the Postgraduate education and teaching reform and practice project of Yangzhou University, grant number JGLX 2021_010, and the Yangzhou Government-Yangzhou University Cooperative Platform Project for Science and Technology Innovation, Grant Number YZ2020262.

Acknowledgments

The authors want to thank the assistance of the Yangzhou University Test Center for providing some of the test instruments and materials.

Conflict of interest

The authors declare that the research was conducted in the absence of any commercial or financial relationships that could be construed as a potential conflict of interest.

Publisher's note

References

Almaali, Y. A., and Al-Busaltan, S. (2021). Permanent deformation characteristics of modified thin overlay bitumen mixtures comprising waste polymers. *Mater. Today Proc.* 42 (5), 2717–2724. doi:10.1016/j.matpr.2020.12.711

ASTM D8225-19 (2019). *Standard test method for determination of cracking tolerance index of asphalt mixture using the indirect tensile cracking test at intermediate temperature*. West Conshohocken, USA: ASTM.

Büchner, J., Wistuba, P. M., Remmler, T., and Wang, D. (2019). On low temperature binder testing using DSR 4 mm geometry. *Mater. Struct.* 52, 113. doi:10.1617/s11527-019-1412-3

Chen, S., Gong, F., Ge, D., You, Z., and Sousa, J. B. (2019). Use of reacted and activated rubber in ultra-thin hot mixture asphalt overlay for wet-freeze climates. *J. Clean. Prod.* 232, 369–378. doi:10.1016/j.jclepro.2019.05.364

Correia, N. S., and Zornberg, J. G. (2018). Strain distribution along geogrid-reinforced asphalt overlays under traffic loading. *Geotext. Geomembr.* 46 (1), 111–120. doi:10.1016/j.geotexmem.2017.10.002

Cui, P., Wu, S., Xiao, Y., Liu, Q., and Wang, F. (2021). Hazardous characteristics and variation in internal structure by hydrodynamic damage of BOF slag-based thin asphalt overlay. *J. Hazard. Mater.* 412, 125344. doi:10.1016/j.jhazmat.2021.125344

Ding, X., Rath, P., Giraldo-Londoño, O., Buttlar, W. G., and Ma, T. (2022). Fracture modeling of rubber-modified binder based on Discrete Element Method. *J. Clean. Prod.* 380, 135017. doi:10.1016/j.jclepro.2022.135017

Gudmarsson, A., Ryden, N., Benedetto, H. D., and Sauzéat, C. (2015). Complex modulus and complex Poisson's ratio from cyclic and dynamic modal testing of asphalt concrete. *Constr. Build. Mater.* 88, 20–31. doi:10.1016/j.conbuildmat.2015.04.007

Guo, Y., Tataranni, P., and Sangiorgi, C. (2023). The use of fibres in asphalt mixtures: a state of the art review. *Constr. Build. Mater.* 390, 131754. doi:10.1016/j.conbuildmat.2023.131754

Han, Y., Zhao, Y., Jiang, J., Ni, F., and Zhao, X. (2021). Effects of design parameters and moisture conditions on interface bond strength between thin friction course (TFC) and underlying asphalt pavements. *Constr. Build. Mater.* 269, 121347. doi:10.1016/j.conbuildmat.2020.121347

Huang, Y., Liu, Z., Liu, L., Zhang, Y., and Xu, Q. (2020). Hybrid modification of Stone mastic asphalt with cellulose and basalt fiber. *Adv. Mater. Sci. Eng.* 2020, 1–11. doi:10.1155/2020/5671256

Ingrassia, L. P., Virgili, A., and Canestrari, F. (2012). Effect of geocomposite reinforcement on the performance of thin asphalt pavements: accelerated pavement testing and laboratory analysis. *Case Stud. Constr. Mater.* 12, e00342. doi:10.1016/j.cscm.2020.e00342

Javilla, B., Fang, H., Mo, L., Shu, B., and Wu, S. (2017). Test evaluation of rutting performance indicators of asphalt mixtures. *Constr. Build. Mater.* 155, 1215–1223. doi:10.1016/j.conbuildmat.2017.07.164

Jin, D., Wang, J., You, L., Ge, D., Liu, C., Liu, H., et al. (2021). Waste cathode-ray-tube glass powder modified asphalt materials: preparation and characterization. *J. Clean. Prod.* 314, 127949. doi:10.1016/j.jclepro.2021.127949

Jin, D., Yin, L., Xin, K., and You, Z. (2023b). Comparison of asphalt emulsion-based chip seal and hot rubber asphalt-based chip seal. *Case Stud. Constr. Mater.* 18, e02175. doi:10.1016/j.cscm.2023.e02175

Jin, T., Liu, L., Yang, R., Sun, L., and Yuan, J. (2023a). Investigation of interlayer bonding performance between asphalt concrete overlay and Portland cement concrete using inclined shear fatigue test. *Constr. Build. Mater.* 400, 132681. doi:10.1016/j.conbuildmat.2023.132681

Jtg, (2011). *Standard test methods of bitumen and bituminous mixtures for highway engineering*. Beijing, China: China Communications Press.

Jtg, (2017). *Specifications for design of highway asphalt pavement*. Beijing, China: China Communications Press.

Jtg, (2019). *Field test methods of highway subgrade pavement*. Beijing, China: China Communications Press.

Li, Y., Zou, Z., Zhang, J., and He, Y. (2023). Study on the evolution of airport asphalt pavement integrated distress based on association rule mining. *Constr. Build. Mater.* 3691, 130565. doi:10.1016/j.conbuildmat.2023.130565

Ling, M., Luo, X., Gu, F., and Lytton, R. L. (2017). Time-temperature-aging-depth shift functions for dynamic modulus master curves of asphalt mixtures. *Constr. Build. Mater.* 157, 943–951. doi:10.1016/j.conbuildmat.2017.09.156

Liu, F., Pan, B., Bian, J., and Zhou, C. (2023). Experimental investigation on the performance of the asphalt mixture with ceramic fiber. *J. Clean. Prod.* 384, 135585. doi:10.1016/j.jclepro.2022.135585

Liu, Z., Luo, S., Quan, X., Wei, X., Yang, X., and Li, Q. (2019). Laboratory evaluation of performance of porous ultra-thin overlay. *Constr. Build. Mater.* 204, 28–40. doi:10.1016/j.conbuildmat.2019.01.147

Lou, K., Xiao, P., Tang, Q., Wu, Y., Wu, Z., and Pan, X. (2022). Research on the micro-nano characteristic of basalt fiber and its impact on the performance of relevant asphalt mastic. *Constr. Build. Mater.* 318, 126048. doi:10.1016/j.conbuildmat.2021.126048

Pei, Z., Lou, K., Kong, H., Wu, B., Wu, X., Xiao, P., et al. (2021). Effects of fiber diameter on crack resistance of asphalt mixtures reinforced by basalt fibers based on digital image correlation Technology. *Materials* 14 (23), 7426. doi:10.3390/ma14237426

Podolsky, J. H., Williams, R. C., and Cochran, E. (2018). Effect of corn and soybean oil derived additives on polymer-modified HMA and WMA master curve construction and dynamic modulus performance. *Int. J. Pavement Res. Technol.* 11 (6), 541–552. doi:10.1016/j.ijprt.2018.01.002

Qin, X., Ma, L., and Wang, H. (2019). Comparison analysis of dynamic modulus of asphalt mixture: indirect tension and uniaxial compression test. *Transp. A* 15, 165–178. doi:10.1080/23249935.2018.1517133

Tan, G., Wang, W., Cheng, Y., Wang, Y., and Zhu, Z. (2020). Master curve establishment and complex modulus evaluation of SBS-modified asphalt mixture reinforced with basalt fiber based on generalized sigmoidal model. *Polymers* 12 (7), 1586. doi:10.3390/polym12071586

Wang, W., Yang, L., Cui, H., Wu, F., Cheng, Y., and Liang, C. (2023). Freeze–thaw damage mechanism analysis of SBS asphalt mixture containing basalt fiber and lignocellulosic fiber based on microscopic void characteristics. *Polymers* 15 (19), 3887. doi:10.3390/polym15193887

Xie, T., and Wang, L. (2023). Optimize the design by evaluating the performance of asphalt mastic reinforced with different basalt fiber lengths and contents. *Constr. Build. Mater.* 363, 129698. doi:10.1016/j.conbuildmat.2022.129698

Xue, X., Zheng, X., Guan, B., Liu, J., Ding, D., Xiong, R., et al. (2022). Long-term skid resistance of high-friction surface treatment of pavement using high-alumina refractory waste. *Constr. Build. Mater.* 351, 128961. doi:10.1016/j.conbuildmat.2022.128961

Yaqub, R., Bandyopadhyay, A., and Ali, H. (2023). Exploring the potential of onboard energy scavenging subsystems for generating valuable data. *Front. Energy Res.* 11, 1259676. doi:10.3389/fenrg.2023.1259676

Zhang, C., Shi, F., Cao, P., and Liu, K. (2022a). The fracture toughness analysis on the basalt fiber reinforced asphalt concrete with prenotched three-point bending beam test. *Case Stud. Constr. Mater.* 16, e01079. doi:10.1016/j.cscm.2022.e01079

Zhang, J., Huang, W., Zhang, Y., Lv, Q., and Yan, C. (2020). Evaluating four typical fibers used for OGFC mixture modification regarding drainage, raveling, rutting and fatigue resistance. *Constr. Build. Mater.* 253, 119131. doi:10.1016/j.conbuildmat.2020.119131

Zhang, M., Zhao, H., Fan, L., and Yi, J. (2022c). Dynamic modulus prediction model and analysis of factors influencing asphalt mixtures using gray relational analysis methods. *J. Mater. Res. Technol.* 19, 1312–1321. doi:10.1016/j.jmrt.2022.05.120

Zhang, Y., Gu, Q., Kang, A., Ding, X., and Ma, T. (2022b). Characterization of mesoscale fracture damage of asphalt mixtures with basalt fiber by environmental scanning electron microscopy. *Constr. Build. Mater.* 344, 128188. doi:10.1016/j.conbuildmat.2022.128188

Zhao, H., Guan, B., Xiong, R., and Zhang, A. (2020). Investigation of the performance of basalt fiber reinforced asphalt mixture. *Appl. Sci.* 10 (5), 1561. doi:10.3390/app10051561